

## Mechanism of White Phosphorus Activation by Three-Coordinate Molybdenum(III) Complexes: A Thermochemical, Kinetic, and Quantum Chemical Investigation

Frances H. Stephens,<sup>†</sup> Marc J. A. Johnson,<sup>†</sup> Christopher C. Cummins,<sup>\*,†</sup>  
Olga P. Kryatova,<sup>‡</sup> Sergey V. Kryatov,<sup>‡</sup> Elena V. Rybak-Akimova,<sup>\*,‡</sup>  
J. Eric McDonough,<sup>§</sup> and Carl D. Hoff<sup>\*,§</sup>

Contribution from the Department of Chemistry, Massachusetts Institute of Technology, 77 Massachusetts Avenue, Cambridge, Massachusetts 02139, Department of Chemistry, Tufts University, 62 Talbot Avenue, Medford, Massachusetts 02155, and Department of Chemistry, University of Miami, 1301 Memorial Drive, Coral Gables, Florida 33146

Received June 28, 2005; E-mail: ccummins@mit.edu

**Abstract:** White phosphorus ( $P_4$ ) reacts with three-coordinate molybdenum(III) trisamides or molybdaziridine hydride complexes to produce either bridging or terminal phosphide ( $P^{3-}$ ) species, depending upon the ancillary ligand steric demands. Thermochemical measurements have been made that place the  $Mo\equiv P$  triple bond dissociation enthalpy at  $92.2 \text{ kcal}\cdot\text{mol}^{-1}$ . Thermochemical measurements together with computational analysis rule out simple P-atom abstraction from  $P_4$  as a step in the phosphorus activation mechanism. Kinetic measurements made by the stopped-flow method show that the reaction between the monomeric molybdenum complexes and  $P_4$  is first-order both in metal complex and in  $P_4$ . *cyclo*- $P_3$  complexes can be obtained when ancillary ligand steric demands are small, but kinetic measurements rule them out as monometallic intermediates in the  $P_4$  activation mechanism. Also studied by calorimetric, kinetic, and in one case variable-temperature NMR methods is the process of  $\mu$ -phosphide bridge formation. Post-rate-determining steps of the  $P_4$  activation process were examined in a search for minima on the reaction's potential energy surface, leading to the proposal of two plausible, parallel, bimetallic reaction channels.

### Introduction

A grand challenge to synthetic chemistry is to find mild metal-mediated or -catalyzed reactions for the direct incorporation of elemental nitrogen ( $N_2$ ) or phosphorus ( $P_4$ ) into organic molecules.<sup>1,2</sup> In the case of elemental nitrogen, breakthroughs of this sort would permit ammonia, the industrial synthesis of which is infrastructure-intensive, to be bypassed as an intermediate.<sup>3</sup> Such breakthroughs also would represent methods for  $^{15}N$ -isotopic labeling from the least expensive source of the isotope:  $^{15}N_2$ . The global phosphorus cycle is analogous to that of nitrogen, with the exception that phosphorus is not an atmospheric element.<sup>4–6</sup> Organophosphorus compounds are synthesized commercially by coke reduction of the phosphate mineral apatite to provide elemental phosphorus as  $P_4$ , which

is purified by distillation and then oxidized with chlorine to  $PCl_3$  prior to salt elimination reactions that yield desirable organophosphorus products.<sup>4–6</sup> Mild metal-mediated or -catalyzed reactions that effect direct incorporation of phosphorus atoms from  $P_4$  into organic molecules would allow the hazardous chlorination process to be avoided, a benefit from the security standpoint, and they also would obviate the salt-generating process and thus provide an environmental benefit.<sup>7–9</sup>

To use elemental phosphorus as a  $P_1$  source in metal-mediated chemical synthesis, metal complexes capable of  $P_4$  activation and breakdown are required. Most transition-element complexes known to bind and activate  $P_4$  yield systems containing  $P_n$  ligands wherein  $n > 1$ . In particular, *cyclo*- $P_3$  and  $P_2$  ligands so derived are well-known.<sup>7–9</sup> In contrast, the three-coordinate molybdenum(III) complex  $Mo(N[t-Bu]Ar)_3$  is known to furnish upon treatment with  $P_4$  the terminal  $P_1$  (phosphide) complex  $PMo(N[t-Bu]Ar)_3$  in essentially quantitative yield.<sup>10,11</sup> This example of metal–phosphorus triple bond and  $P_1$  ligand generation upon  $P_4$  activation by a metal complex is unique.

<sup>†</sup> Massachusetts Institute of Technology.

<sup>‡</sup> Tufts University.

<sup>§</sup> University of Miami.

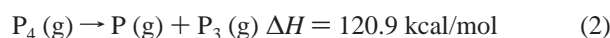
- (1) Smaglik, P. *Nature* **2000**, *406*, 807–808.
- (2) Lippard, S. J. *Chem. Eng. News* **2000**, *78*, 64–65.
- (3) Henderickx, H.; Kwakkenbos, G.; Peters, A.; van der Spoel, J.; de Vries, K. *Chem. Commun.* **2003**, 2050–2051.
- (4) Emsley, J.; Hall, D. *The chemistry of phosphorus: environmental, organic, inorganic, biochemical and spectroscopic aspects*; Harper and Row: London; New York, 1976.
- (5) Emsley, J. *Nature's building blocks: an A-Z guide to the elements*; Oxford University Press: Oxford; New York, 2001.
- (6) Emsley, J. *The 13th element: the sordid tale of murder, fire and phosphorus*; John Wiley & Sons: New York, 2000.

- (7) Barbaro, P.; Ienco, A.; Mealli, C.; Peruzzini, M.; Scherer, O.; Schmitt, G.; Vizza, F.; Wolmershauser, G. *Chem. Eur. J.* **2003**, *9*, 5195–5210.
- (8) Peruzzini, M.; Abdreimova, R.; Budnikova, Y.; Romerosa, A.; Scherer, O.; Sitzmann, H. *J. Organomet. Chem.* **2004**, *689*, 4319–4331.
- (9) Ehses, M.; Romerosa, A.; Peruzzini, M. *Top. Curr. Chem.* **2002**, *220*, 107–140.
- (10) Laplaza, C. E.; Davis, W. M.; Cummins, C. C. *Angew. Chem., Int. Ed. Engl.* **1995**, *34*, 2042–2044.

Steric effects are clearly key in determining the reaction's outcome, as the smaller "Mo(N[*i*-Pr]Ar)<sub>3</sub>" fragment, available in the form of its isomeric molybdaziridine-hydride synthon Mo(H)(η<sup>2</sup>-Me<sub>2</sub>C=NAr)(N[*i*-Pr]Ar)<sub>2</sub>,<sup>12,13</sup> yields either a P<sub>1</sub>-bridged dimetallic complex or a *cyclo*-P<sub>3</sub>-containing mononuclear system upon P<sub>4</sub> treatment, depending upon the reaction conditions.

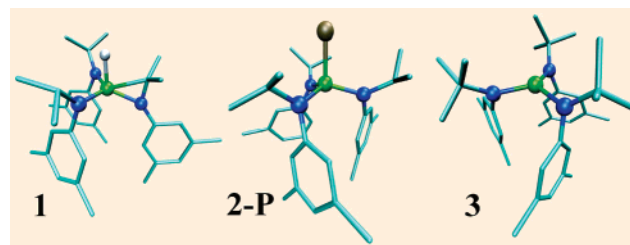
Because the latter reactions are clean and take place rapidly under mild reaction conditions, an ideal opportunity for detailed mechanistic scrutiny was presented. In stark contrast to the situation with N<sub>2</sub>,<sup>14–16</sup> mechanistic scrutiny of P<sub>4</sub>-activation reactions has been essentially absent from the literature despite the fact that, like nitrogen, the element phosphorus is necessary for life and is of tremendous economic importance.<sup>4–6</sup> With the work presented herein we offer a thermochemical and kinetic analysis of P<sub>4</sub>-activation reactions effected by molybdenum complexes, an analysis that places clear boundaries on the possible operative mechanisms.

An important guide to possible modes of P<sub>4</sub> activation can be gained from the thermochemistry of various P<sub>*n*</sub> fragments; ΔH<sup>o</sup><sub>f</sub> (kcal/mol): P<sub>4</sub>(g) = 14.1; P<sub>3</sub>(g) = 59.4; P<sub>2</sub>(g) = 34.4; P(g) = 75.6 kcal/mol.<sup>17,18</sup> Key derived enthalpies for different fragmentation modes of P<sub>4</sub> are shown in eqs 1–4 below. Metal complex interactions with P<sub>4</sub> in which reactive P<sub>*n*</sub> fragments are ejected will require that the L<sub>*n*</sub>M–P<sub>4–*n*</sub> interaction is sufficiently strong to overcome the thermochemical barriers shown in eqs 1–4.



The complex Mo(H)(η<sup>2</sup>-Me<sub>2</sub>C=NAr)(N[*i*-Pr]Ar)<sub>2</sub> (**1**), its tautomer "Mo(N[*i*-Pr]Ar)<sub>3</sub>" (**2**), and also the bona fide three-coordinate molybdenum(III) complex Mo(N[*t*-Bu]Ar)<sub>3</sub> (**3**) all are good candidates to have sufficient activity to engender P<sub>4</sub> binding and subsequent generation of reactive P<sub>*n*</sub> fragments. Although isopropyl-substituted complex **1** exists as the formally five-coordinate molybdaziridine-hydride,<sup>12</sup> its reactivity with additional ligands parallels that of the bona fide three-coordinate molybdenum(III) complex **3** and thus yields derivatives of the tris-*N*-isopropylanilide fragment **2**.<sup>13</sup> The molybdaziridine-hydride functional group in **1** effectively masks via a reversible cyclometalation process an open coordination site to be made available for P<sub>4</sub> binding.<sup>13</sup> Despite their similar reactivity patterns, the complexes **1** and **3** also display differences (Chart 1). For example, there is an increased proclivity toward η<sup>2</sup>-

**Chart 1.** Three of the Key Molecules Involved in This Study as Drawn from Crystallographic Coordinates; Blue, N; Green, Mo; White, H; Mauve, P



substrate binding displayed by the less sterically hindered isopropyl derivative.<sup>19–21</sup>

Both **1** and **3** react under mild conditions with molecular N<sub>2</sub>,<sup>12,22–26</sup> and with white phosphorus (P<sub>4</sub>).<sup>10–12,26,27</sup> Mechanistic and computational studies of the dinitrogen cleavage reaction effected by **3** have established that the process is a bimetallic one in which an N<sub>2</sub> ligand serving as a bridge between two Mo centers is pulled apart homolytically.<sup>23,28–33</sup> A key focus of the present work is to discern whether a bimetallic mechanism is similarly operative for P<sub>4</sub> cleavage by complexes **1** and/or **3**.

## Experimental Section

**General Considerations for Synthetic Procedures.** Unless otherwise stated, all operations were performed in a Vacuum Atmospheres drybox under an atmosphere of purified nitrogen or using Schlenk techniques under an argon atmosphere. Compounds HMo(η<sup>2</sup>-Me<sub>2</sub>C=NAr)(N[*i*-Pr]Ar)<sub>2</sub> (**1**),<sup>12</sup> (μ-P)[Mo(N[*i*-Pr]Ar)<sub>3</sub>]<sub>2</sub> ((μ-P)**2**),<sup>26</sup> and PMo(N[*i*-Pr]Ar)<sub>3</sub> (**2-P**),<sup>26,27</sup> Mo(N[*t*-Bu]Ar)<sub>3</sub> (**3**),<sup>21,23,34</sup> and PMo(N[*t*-Bu]Ar)<sub>3</sub> (**3-P**),<sup>10</sup> were prepared as described previously. Diethyl ether, *n*-pentane, dichloromethane, and toluene were dried and deoxygenated using a procedure described in the literature.<sup>35</sup> Benzene-*d*<sub>6</sub> and dichloromethane-*d*<sub>2</sub> were degassed and dried over 4 Å molecular sieves. Cyclohexanol was vacuum distilled from sodium. Celite, alumina, and 4 Å molecular sieves were dried in vacuo overnight at a temperature above 200 °C. <sup>1</sup>H, <sup>2</sup>H, <sup>13</sup>C, and <sup>31</sup>P NMR spectra were recorded on Varian Mercury-300 or Varian INOVA-500 spectrometers. <sup>1</sup>H and <sup>13</sup>C chemical shifts are reported with respect to internal solvent resonances

- (11) Wu, G.; Rovnyak, D.; Johnson, M. J. A.; Zanetti, N. C.; Musaev, D. G.; Morokuma, K.; Schrock, R. R.; Griffin, R. G.; Cummins, C. C. *J. Am. Chem. Soc.* **1996**, *118*, 10654–10655.
- (12) Tsai, Y. C.; Johnson, M. J. A.; Mindiola, D. J.; Cummins, C. C.; Klooster, W. T.; Koetzle, T. F. *J. Am. Chem. Soc.* **1999**, *121*, 10426–10427.
- (13) Stephens, F. H.; Figueroa, J. S.; Cummins, C. C.; Kryatova, O. P.; Kryatov, S. V.; Rybak-Akimova, E. V.; McDonough, J. E.; Hoff, C. D. *Organometallics* **2004**, *23*, 3126–3138.
- (14) MacKay, B. A.; Fryzuk, M. D. *Chem. Rev.* **2004**, *104*, 385–401.
- (15) Shaver, M. P.; Fryzuk, M. D. *Adv. Synth. Catal.* **2003**, *345*, 1061–1076.
- (16) Fryzuk, M. D.; Johnson, S. A. *Coord. Chem. Rev.* **2000**, *200*, 379–409.
- (17) Bennett, S. L.; Margrave, J. L.; Franklin, J. L. *J. Chem. Phys.* **1974**, *61*, 1647–1651.
- (18) NIST Chemistry WebBook. <http://webbook.nist.gov>.

- (19) Tsai, Y. C.; Diaconescu, P. L.; Cummins, C. C. *Organometallics* **2000**, *19*, 5260–5262.
- (20) Blackwell, J. M.; Figueroa, J. S.; Stephens, F. H.; Cummins, C. C. *Organometallics* **2003**, *22*, 3351–3353.
- (21) Tsai, Y. C.; Stephens, F. H.; Meyer, K.; Mendiratta, A.; Gheorghiu, M. D.; Cummins, C. C. *Organometallics* **2003**, *22*, 2902–2913.
- (22) Laplaza, C. E.; Cummins, C. C. *Science* **1995**, *268*, 861–863.
- (23) Laplaza, C. E.; Johnson, M. J. A.; Peters, J. C.; Odom, A. L.; Kim, E.; Cummins, C. C.; George, G. N.; Pickering, I. J. *J. Am. Chem. Soc.* **1996**, *118*, 8623–8638.
- (24) Peters, J. C.; Cherry, J. P. F.; Thomas, J. C.; Baraldo, L.; Mindiola, D. J.; Davis, W. M.; Cummins, C. C. *J. Am. Chem. Soc.* **1999**, *121*, 10053–10067.
- (25) Tsai, Y. C.; Cummins, C. C. *Inorg. Chim. Acta* **2003**, *345*, 63–69.
- (26) Cherry, J. P. F.; Stephens, F. H.; Johnson, M. J. A.; Diaconescu, P. L.; Cummins, C. C. *Inorg. Chem.* **2001**, *40*, 6860.
- (27) Stephens, F. H.; Figueroa, J. S.; Diaconescu, P. L.; Cummins, C. C. *J. Am. Chem. Soc.* **2003**, *125*, 9264–9265.
- (28) Cui, Q.; Musaev, D. G.; Svensson, M.; Sieber, S.; Morokuma, K. *J. Am. Chem. Soc.* **1995**, *117*, 12366–12367.
- (29) Hahn, J.; Landis, C. R.; Nasluzov, V. A.; Neyman, K. M.; Rosch, N. *Inorg. Chem.* **1997**, *36*, 3947–3951.
- (30) Neyman, K. M.; Nasluzov, V. A.; Hahn, J.; Landis, C. R.; Rosch, N. *Organometallics* **1997**, *16*, 995–1000.
- (31) Christian, G.; Stranger, R.; Yates, B. F.; Graham, D. C. *Dalton Trans.* **2005**, 962–968.
- (32) Christian, G.; Stranger, R. *Dalton Trans.* **2004**, 2492–2495.
- (33) Christian, G.; Driver, J.; Stranger, R. *Faraday Discuss.* **2003**, *124*, 331–341.
- (34) Laplaza, C. E.; Odom, A. L.; Davis, W. M.; Cummins, C. C.; Protasiewicz, J. D. *J. Am. Chem. Soc.* **1995**, *117*, 4999–5000.
- (35) Pangborn, A. B.; Giardello, M. A.; Grubbs, R. H.; Rosen, R. K.; Timmers, F. J. *Organometallics* **1996**, *15*, 1518–1520.

(C<sub>6</sub>D<sub>6</sub>, 7.16 and 128.39 ppm). <sup>2</sup>H NMR spectra are referenced to an external reference (C<sub>6</sub>D<sub>6</sub> in Et<sub>2</sub>O, 7.16 ppm). <sup>31</sup>P chemical shifts are reported with respect to external reference (85% H<sub>3</sub>PO<sub>4</sub>, 0.0 ppm). X-ray data collections were carried out on a Siemens Platform three-circle diffractometer with a CCD detector using Mo K $\alpha$  radiation  $\lambda = 0.71073$  Å. All software used for diffraction data processing and crystal-structure solution and refinement are contained in the SAINT<sup>+</sup> (v6.45) and SHELXTL (v6.14) program suites, respectively (G. Sheldrick, Bruker AXS, Madison, WI).

**Synthesis of ( $\eta^3$ -P<sub>3</sub>)Mo(N[*i*-Pr]Ar)<sub>3</sub>, 2–P<sub>3</sub>.** White phosphorus (0.417 g, 3.369 mmol, 0.98 equiv) was dissolved in 45 mL of toluene. Orange-brown **1** (2.013 g, 3.455 mmol) was dissolved in 30 mL of toluene. The latter solution was added dropwise over ca. 20 min to the former, whereupon the mixture was cooled to –35 °C overnight, resulting in the formation of yellow, fibrous ( $\eta^3$ -P<sub>3</sub>)Mo(N[*i*-Pr]Ar)<sub>3</sub> (1.326 g, 1.963 mmol, 56.8%). <sup>1</sup>H NMR (C<sub>6</sub>D<sub>6</sub>, 300 MHz):  $\delta = 6.69$  (s, 3H, para), 6.54 (br s, 6H, ortho), 4.82 (br, 3H, methine), 2.15 (s, 18H, aryl methyl), 1.23 (d, 18H) ppm. <sup>13</sup>C NMR (125 MHz, CD<sub>2</sub>Cl<sub>2</sub>):  $\delta = 150.16$  (s, ipso), 137.42 (s, meta), 128.42 (d, para), 128.35 (d, ortho), 60.14 (d, methine), 22.24 (m, *i*-Pr methyl), 21.59 (q, aryl methyl) ppm. <sup>31</sup>P NMR (75 MHz, C<sub>6</sub>D<sub>6</sub>):  $\delta = -185$  ppm. Anal. Calcd. for C<sub>33</sub>H<sub>48</sub>N<sub>3</sub>MoP<sub>3</sub>: C, 57.14; H, 6.97; N, 6.06. Found: C, 57.92; H, 7.23; N, 5.83.

**Synthesis of ( $\eta^3$ -P<sub>3</sub>)Mo(OCy)<sub>3</sub>·HN(*i*-Pr)Ar.** Using 50 mL of toluene, a solution of 2–P<sub>3</sub> (0.190 g, 0.260 mmol) and cyclohexanol (0.086 g, 0.855 mmol, 3.3 equiv) was prepared. The solution was heated to 60 °C overnight. The reaction mixture was filtered and the solvent was removed in vacuo. The residue was extracted with pentane and the product was crystallized from the extract at –35 °C (0.070 g, 0.107 mmol, 41%). <sup>1</sup>H NMR (300 MHz, C<sub>6</sub>D<sub>6</sub>):  $\delta = 6.42$  (s, 1H, para), 6.17 (s, 2H, ortho), 4.79 (septet, 3H, cyclohexyl quaternary), 3.42 (septet, 1H methine), 2.95 (br d, 1H, amine), 2.23 (s, 6H, aryl methyl), 1.90 (br, cyclohexyl), 1.58 (br, cyclohexyl), 1.50 (br, cyclohexyl), 1.22 (br, cyclohexyl), 0.95 (d, 6H, *i*-Pr methyl) ppm. <sup>31</sup>P NMR (121 MHz, C<sub>6</sub>D<sub>6</sub>):  $\delta = -185$  ppm. Note: while this <sup>31</sup>P chemical shift is the same as that for precursor 2–P<sub>3</sub>, the signal for the latter is distinguishable as it is quite broad while that for ( $\eta^3$ -P<sub>3</sub>)Mo(OCy)<sub>3</sub>·HN(*i*-Pr)Ar is sharp, only ca. 5 Hz at half-width. Anal. Calcd. for C<sub>29</sub>H<sub>50</sub>MoNO<sub>3</sub>P<sub>3</sub>: C, 53.62; H, 7.76; N, 2.15. Found: C, 53.83; H, 7.95; N, 2.17.

**Stopped-flow kinetic measurements** were performed using a Hi-Tech Scientific (Salisbury, Wiltshire, UK) SF-43 Multi-Mixing Cryo-Stopped-Flow Instrument, in a single-mixing mode of the instrument with a 1:1 (v/v) ratio, as described in detail elsewhere.<sup>13</sup> Reactions corresponding to eqs 7 through 11 were studied in a diode array mode using Xenon arc lamp in the following temperature intervals: from 30 to 60 °C (Reaction 7); from –30 to –10 °C (Reaction 8); from 5 to 50 °C (Reaction 9); from –50 to 10 °C (Reaction 10); from –5 to 60 °C (Reaction 11). Second-order conditions were applied, with the concentration of the reactant solutions ranging from 0.12 to 0.6 mM. Reaction 5 was studied over the temperature range –5 to 40 °C under pseudo-first-order conditions, varying the concentration of **1** from 0.15 to 1.2 mM (before mixing) and the concentration of P<sub>4</sub> from 0.075 to 6.0 mM (before mixing). Reaction 6 gave good data only in the temperature range –50 to –20 °C and was observed to produce colored impurities at higher temperatures. The reaction was studied using an excess of complex **3** (8 [3]: [P<sub>4</sub>]) and under pseudo-first-order conditions ([3] = 0.6 mM, [P<sub>4</sub>] = 6 mM, before mixing). In addition to acquiring time-resolved spectral changes, the reactions using P<sub>4</sub> (eqs 5 and 6) were followed at single wavelengths (visible lamp) to avoid decomposition of white phosphorus upon exposure to UV light.

**Calorimetric Measurements.** Enthalpies of reaction were measured using a Setaram C-80 Calvet calorimeter. White phosphorus was sublimed in high vacuum, recrystallized from toluene, and then resublimed to obtain pure white crystalline material which was stored in the glovebox shielded from light. In a typical procedure, the calorimeter cell and components were dried in an oven at 120 °C for

an hour and then taken into the glovebox. A solution of 0.50 g of **3** in 5.0 mL of freshly distilled toluene was added to the solution holder, and 9.0 mg of P<sub>4</sub> was loaded into a high-density polyethylene cup mated to a stainless steel tapered plug welded to a thin rod which exited the calorimeter through a sealed fitting. The calorimeter vessel was sealed in the glovebox and loaded into the calorimeter. Following temperature equilibration, reaction was initiated by pulling the rod upward to release the polyethylene cup and then rotating the calorimeter to allow complete mixing. The enthalpy of reaction,  $-19.5 \pm 0.7$  kcal/mol is the average of six individual measurements.

## Results and Discussion

**Synthesis of *cyclo*-P<sub>3</sub> Complexes.** Interestingly, the outcome of the reaction of molybdaziridine–hydride **1** with P<sub>4</sub> is very sensitive to the employed reaction conditions. While as reported previously the reaction of **1** with P<sub>4</sub> (added to the reaction mixture as solid pieces) in ether, a solvent in which P<sub>4</sub> has limited solubility, leads to formation of the  $\mu$ -phosphide complex 2<sub>2</sub>– $\mu$ -P in high yield,<sup>26</sup> we find that carrying out the reaction by adding a toluene solution of **1** to a toluene solution of excess P<sub>4</sub> leads instead to the formation of a *cyclo*-P<sub>3</sub> complex. The *cyclo*-P<sub>3</sub> complex ( $\eta^3$ -P<sub>3</sub>)Mo(N[*i*-Pr]Ar)<sub>3</sub>, 2–P<sub>3</sub>, is obtained as a fibrous, yellow solid and is associated with a <sup>31</sup>P NMR singlet at  $\delta = -185$  ppm, close in chemical shift to that observed for Chisholm's related complex ( $\eta^3$ -P<sub>3</sub>)W(ONP)<sub>3</sub>(HNMe<sub>2</sub>).<sup>36</sup> The <sup>31</sup>P NMR signal for the latter is found at  $\delta = -205$  ppm, and the dimethylamine ligand is located trans to the *cyclo*-P<sub>3</sub> ligand in this pseudo-C<sub>3</sub> symmetric, crystallographically characterized tungsten complex.<sup>36</sup>

The possibility should be considered that 2–P<sub>3</sub> may be an intermediate in the synthesis of 2<sub>2</sub>– $\mu$ -P. For this reason, 5 equiv of **1** were treated with 2–P<sub>3</sub> with the result that 3 equiv of 2<sub>2</sub>– $\mu$ -P were quantitatively formed. While this result is consistent with the intermediacy of 2–P<sub>3</sub> in the synthesis of 2<sub>2</sub>– $\mu$ -P, kinetic studies described below serve to rule out this possibility.

Because it did not prove possible to characterize 2–P<sub>3</sub> via single-crystal X-ray diffraction methods, a derivative was sought. Said derivative was obtained by treatment of 2–P<sub>3</sub> with 3 equiv of cyclohexanol, the idea being replacement of the three N(*i*-Pr)Ar ligands with cyclohexanoxide ligands via alcoholysis. The reaction led to isolation of ( $\eta^3$ -P<sub>3</sub>)Mo(OCy)<sub>3</sub>(HN[*i*-Pr]Ar), quite analogous to known ( $\eta^3$ -P<sub>3</sub>)W(ONP)<sub>3</sub>(HNMe<sub>2</sub>),<sup>36</sup> and this molybdenum–P<sub>3</sub> complex was fully characterized, including a single-crystal X-ray diffraction study (Figure 1). A similar alcoholysis strategy has been successful in the synthesis of PMo(O-1-MeCy)<sub>3</sub>,<sup>27</sup> and also in the synthesis of molybdenum alkylidyne complexes useful as alkyne metathesis catalysts.<sup>19,20,37–39</sup> Note that the ROH-stable [P<sub>3</sub>Mo]<sup>3+</sup> core can be considered portable<sup>40</sup> and could conceivably be transferred to a variety of supporting ligand frameworks by similar protonolysis reactions of ( $\eta^3$ -P<sub>3</sub>)Mo(N[*i*-Pr]Ar)<sub>3</sub>, 2–P<sub>3</sub>, reactions in which 3 equiv of the amine HN(*i*-Pr)Ar are evolved.

**Kinetics of P<sub>4</sub> Activation by **1**.** Pseudo-first-order conditions were employed with a 10–40-fold excess of P<sub>4</sub>, and the

(36) Chisholm, M. H.; Huffman, J. C.; Pasterczyk, J. W. *Inorg. Chim. Acta* **1987**, *133*, 17–18.

(37) Zhang, W.; Kraft, S.; Moore, J. S. *J. Am. Chem. Soc.* **2004**, *126*, 329–335.

(38) Zhang, W.; Kraft, S.; Moore, J. S. *Chem. Commun.* **2003**, 832–833.

(39) Furstner, A.; Mathes, C.; Lehmann, C. W. *Chem. Eur. J.* **2001**, *7*, 5299–5317.

(40) Cherry, J. P. F.; Diaconescu, P. L.; Cummins, C. C. *Can. J. Chem.* **2005**, *83*, 302–307.

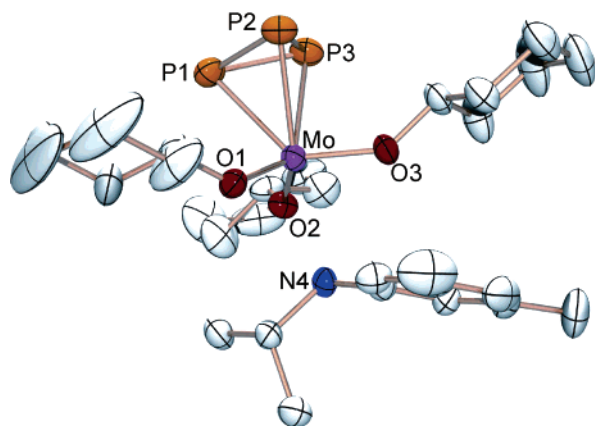
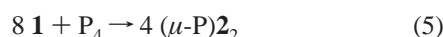


**Figure 1.** Thermal ellipsoid drawing at 50% probability of  $(\eta^3\text{-P}_3)\text{Mo}(\text{OCy})_3(\text{HN}[i\text{-Pr]Ar})$ .

observed kinetic data, an absorbance increase at 500 nm corresponding to formation of the phosphide-bridged complex  $(\mu\text{-P})_2$ , gave a good fit to a first-order kinetic equation (Figures S1–S3). The kinetic observable<sup>41</sup> corresponds to the following overall reaction:

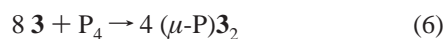


Indeed, varying the initial concentration of **1** while keeping the concentration of  $\text{P}_4$  large and constant yielded identical values of the pseudo-first-order rate constant  $k_{\text{obs}}$ . This confirms that the reaction rate depends on the first power of **[1]**. A plot of  $k_{\text{obs}}$  vs the initial concentration of  $\text{P}_4$  was a straight line with a small intercept (ca. 25%) as shown in Figure S3. Thus, the reaction is essentially irreversible and is first order in  $\text{P}_4$ . Consequently, activation of  $\text{P}_4$  by **1** is a second-order process with the following rate law:

$$v = k_{\text{obs}}[\mathbf{1}] = k_2[\mathbf{1}][\text{P}_4]$$

Activation parameters obtained for this  $\text{P}_4$  activation by **1** are consistent with the inferred bimolecular nature of the process with  $\Delta H^\ddagger = 6.0 \pm 0.5 \text{ kcal}\cdot\text{mol}^{-1}$ , a low activation enthalpy, and  $\Delta S^\ddagger = -30 \pm 4 \text{ eu}$ . Collected in Table 1 are kinetic parameters for this and other reactions analyzed in the course of this study.

**Kinetics of  $\text{P}_4$  Activation by **3**.** At low temperature in the stopped-flow apparatus the activation of  $\text{P}_4$  by **3** is kinetically similar to activation by **1** and proceeds according to the following equation:

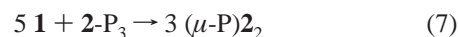


While the mononuclear terminal phosphide  $\text{PMo}(\text{N}[t\text{-Bu}]\text{Ar})_3$ , **3-P**, is the primary product of  $\text{P}_4$  activation by **3** at room temperature in the synthetic preparation of **3-P**,<sup>10</sup> below  $-20^\circ\text{C}$  **3-P** is seen to combine rapidly with **3** to provide the dinuclear  $\mu$ -phosphide  $(\mu\text{-P})_3$  as a readily observed chromophore (Figures S4–S5).

Overall, the reaction of eq 6 is first order in  $\text{P}_4$  and first order in molybdenum complex **3**. While the activation parameters obtained from kinetic study of this process as a function of

temperature ( $\Delta H^\ddagger = 4.4 \pm 0.8 \text{ kcal}\cdot\text{mol}^{-1}$ ,  $\Delta S^\ddagger = -37 \pm 6 \text{ eu}$ , Figure S6) are roughly similar to those obtained for the analogous  $\text{P}_4$  activation by **1** (eq 5), it is seen that the process is several times faster for three-coordinate **3** than for molybdaziridine–hydride **1**. While the rates are not directly comparable because the process involving three-coordinate **3** was of necessity measured in a lower temperature regime,<sup>42</sup> we can compare the extrapolated second-order rate constant  $k_2$  for eq 5 ( $k_2 = 2 \text{ M}^{-1} \text{ s}^{-1}$ ) at  $-20^\circ\text{C}$  with that measured directly for eq 6 at the same temperature ( $k_2 = 6 \text{ M}^{-1} \text{ s}^{-1}$ ). At  $-10^\circ\text{C}$  this comparison is as follows: complex **1**,  $k_2 = 3.5 \text{ M}^{-1} \text{ s}^{-1}$ ; complex **3**,  $k_2 = 26 \text{ M}^{-1} \text{ s}^{-1}$ . Mechanistically this kinetic difference can be interpreted in terms of the greater reorganization requirement for molybdaziridine–hydride **1**, as compared with simple  $\text{P}_4$ -binding for three-coordinate **3**. In essence, with its open coordination site, three-coordinate **3** is already “prepared” for  $\text{P}_4$  binding/activation.

**Mechanistic Role of the *cyclo*- $\text{P}_3$  Complex.** Compound **2-P**<sub>3</sub> is found to react cleanly with molybdaziridine–hydride **1** (Figure S7) to form the bridged phosphide complex  $(\mu\text{-P})_2$  as follows:



This being the case, the question arises as to the kinetic viability of **2-P**<sub>3</sub> as an intermediate in the  $\text{P}_4$  activation by molybdaziridine–hydride **1**. In telling fashion, the reaction of eq 7 was found to be the slowest of all the reactions studied in this work. On this basis **2-P**<sub>3</sub> can be excluded as an intermediate in  $\text{P}_4$  activation. The reaction of **1** with **2-P**<sub>3</sub> must necessarily proceed via several steps along the way to final products. Whatever the nature of these steps, they all occurred significantly faster than the rate-limiting step, and no intermediate complexes were observed in the course of carrying out the stopped-flow experiments (Figure S7). Between  $30$  and  $60^\circ\text{C}$  under second-order conditions, the data gave a good fit to a second-order kinetic equation, first-order both in **2-P**<sub>3</sub> and in **1**.

The kinetic data are thus in accord with a rate-limiting binding of **2-P**<sub>3</sub> by **1**. Activation parameters for the reaction ( $\Delta H^\ddagger = 10.5 \pm 0.5 \text{ kcal}\cdot\text{mol}^{-1}$ ,  $\Delta S^\ddagger = -17 \pm 2 \text{ eu}$ ) further reveal a higher activation enthalpy than is needed for a direct reaction between **1** and  $\text{P}_4$ .

**Formation of the Phosphide Bridge.** To understand the overall reaction mechanism of  $\text{P}_4$  activation in these systems it is helpful to consider the pathway(s) by which  $\mu$ -phosphide bridges may arise. Note also that the structurally characterized members of this family are low-spin ( $S = 1/2$ ) and have inversion symmetry at the bridging phosphorus atom, in addition to Mo–P multiple bond character.<sup>26,43</sup> The  $\mu$ -phosphide complexes  $(\mu\text{-P})_2$  and  $(\mu\text{-P})_3$  also provide the principal chromophores for which concentration changes are followed in this work’s stopped-flow kinetic studies. Formation of the  $(\mu\text{-P})_3$  dinuclear complex by combination of **3** with **3-P** is an equilibrium process:



(41) Any *cyclo*- $\text{P}_3$  complex formed under these conditions is excluded from the kinetic analysis as the chromophore under observation is the phosphide-bridged dimolybdenum product.

(42) At temperatures above  $-20^\circ\text{C}$  colored impurities were produced and were found to interfere with kinetic measurements.

(43) Johnson, M. J. A.; Lee, P. M.; Odom, A. L.; Davis, W. M.; Cummins, C. C. *Angew. Chem., Int. Ed. Engl.* **1997**, *36*, 87–91.

**Table 1.** Activation Parameters for Reactions Corresponding to Eqs 5–11

	1 + P <sub>4</sub> eq 5	3 + P <sub>4</sub> eq 6	1 + 2-η <sup>3</sup> -P <sub>3</sub> eq 7	3 + 3-P eq 8	1 + 2-P eq 9	3 + 2-P eq 10	1 + 3-P eq 11
E <sub>a</sub> (kcal·mol <sup>-1</sup> )	6.7 ± 0.5	5.1 ± 0.8	11.2 ± 0.5	4 ± 1	11.2 ± 0.5	3.2 ± 0.4	9.5 ± 0.5
ΔH <sup>‡</sup> (kcal·mol <sup>-1</sup> )	6.0 ± 0.5	4.4 ± 0.8	10.5 ± 0.5	3.3 ± 1	10.5 ± 0.5	2.7 ± 0.4	8.7 ± 0.5
ΔS <sup>‡</sup> (eu)	-30 ± 4	-37 ± 6	-17 ± 2	-38 ± 8	-11 ± 2	-33 ± 4	-22 ± 4
k <sub>2</sub> , M <sup>-1</sup> s <sup>-1</sup> , 60 °C	<i>415.4<sup>a</sup></i>	<i>b</i>	166.7	<i>c</i>	2533.3	6623 <sup>a</sup>	400
k <sub>2</sub> , M <sup>-1</sup> s <sup>-1</sup> , 25 °C	126.7	<i>b</i>	23	<i>c</i>	280	3733.3	57.8
k <sub>2</sub> , M <sup>-1</sup> s <sup>-1</sup> , 5 °C	57	<i>a</i>	5.9 <sup>a</sup>	<i>b</i>	73.7 <sup>a</sup>	2444.4	17.8
k <sub>2</sub> , M <sup>-1</sup> s <sup>-1</sup> , -5 °C	36.7	11 <sup>a</sup>	2.8 <sup>a</sup>	51	34.8 <sup>a</sup>	1955.6	10.7

<sup>a</sup> Rate constants calculated from Eyring plots are italicized, and those measured directly are in standard font. <sup>b</sup> The reaction was studied at lower temperatures (from -50 to -20 °C). Extrapolation over a broad temperature range is considered unreliable. <sup>c</sup> The reaction was studied at lower temperature (from -30 to -10 °C). Extrapolation over broad temperature range is considered unreliable.

This equilibrium is shifted to the right at low temperature, but below -30 °C the process becomes too slow for the stopped-flow technique. The data obtained between -30 °C and -10 °C under second-order conditions show a very clean process (Figure S8) that allowed for an estimation of activation parameters as follows: ΔH<sup>‡</sup> = 3.3 ± 1 kcal·mol<sup>-1</sup>, ΔS<sup>‡</sup> = -38 ± 8 eu (Table 1, Figure S9). The combination reaction represented by eq 8 is at least twice as fast as the rate-limiting step for P<sub>4</sub> activation by **3** over the studied temperature range.

Equilibrium 8 was also studied using variable-temperature <sup>2</sup>H NMR measurements using the d<sub>6</sub>-labeled variant of the *N*-*tert*-butylanilide ligand.<sup>44</sup> Deuterium NMR analysis of a 1:1 mixture of P≡Mo(N[C(CH<sub>3</sub>)(CD<sub>3</sub>)<sub>2</sub>]Ar)<sub>3</sub> (**3**-P-d<sub>18</sub>, <sup>2</sup>H NMR: δ = 2 ppm) and **3**-d<sub>18</sub> (<sup>2</sup>H NMR: δ = 70 ppm) revealed an equilibrium between the starting materials and **3**<sub>2</sub>-μ-P (<sup>2</sup>H NMR: δ = 8 ppm). At ca. 30 °C, more than 90% of the mixture was in the form of the reactants, whereas at -35 °C more than 90% of the mixture was **3**<sub>2</sub>-μ-P. An examination of the temperature dependence of the equilibrium constant (K<sub>eq</sub>) permitted determination of the thermodynamic parameters of the μ-phosphide bridge formation process. The ΔH<sub>rxn</sub> is -20.7-(4) kcal·mol<sup>-1</sup> and ΔS<sub>rxn</sub> is -69.4(15) eu. The very negative reaction entropy is attributable to the loss of rotational degrees of freedom involving bonds to the ligand nitrogen atoms. The previously reported X-ray crystal structure of the -N(*t*-Bu)Ph analogue of **3**<sub>2</sub>-μ-P shows enmeshed *t*-Bu groups.<sup>43</sup> The rotational freedom in **3**<sub>2</sub>-μ-P is decreased to such an extent that <sup>1</sup>H NMR spectroscopy revealed two environments for the ligands' aryl groups (six equivalent aryl rings each with two *ortho* and two aryl methyl singlets). This is consistent with the freezing out of the molecule into a C<sub>1</sub>-symmetric structure as observed in the solid state,<sup>43</sup> with rocking about the Mo-N bonds completely stopped. In the solid-state structure of (μ-P)-{Mo(N[*t*-Bu]Ph)<sub>3</sub>}<sub>2</sub>,<sup>43</sup> the factor leading to two inequivalent aryl *ortho* environments is the P-Mo-N-C dihedral angle averaging 33°, together with the average aryl group/amido plane dihedral of ca. 90°. Most C<sub>3</sub>-symmetric XMo(N[*t*-Bu]Ar)<sub>3</sub> (e.g., X = N or P) molecules exhibit a single aryl *ortho* <sup>1</sup>H NMR signal at 25 °C because interconversion of the C<sub>3</sub>-symmetric enantiomers, either through a C<sub>3v</sub> transition state or by a stepwise gearing process,<sup>45</sup> is facile.

Also studied by stopped-flow kinetic methods were the three other possible combination reactions involving fragments **2** and **3** that lead to μ-phosphide complexes:

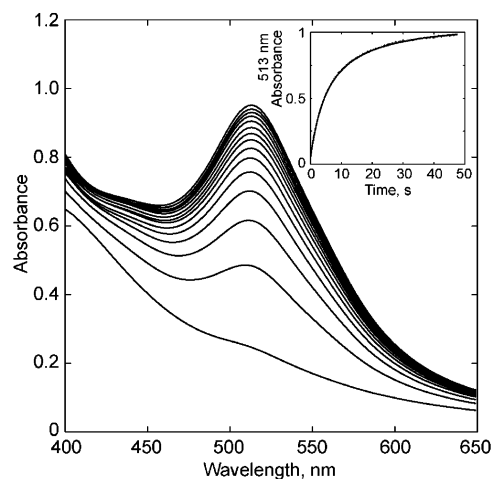
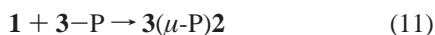
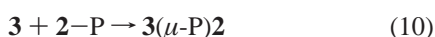


**Figure 2.** Time-resolved (2.5 s intervals) spectral changes and a kinetic trace at 513 nm overlaid with a second-order fit obtained upon mixing of 0.15 mM toluene solutions of **2**-P and **3** in the stopped-flow apparatus at 10 °C.

Unlike the most hindered μ-phosphide system described above, namely (μ-P)**3**<sub>2</sub>, with its six *tert*-butyl groups surrounding the bridging phosphorus atom in the molecule's equatorial girdle,<sup>43</sup> the μ-phosphide complexes (μ-P)**2**<sub>2</sub> and **3**(μ-P)**2** are formed essentially irreversibly. This allowed the kinetics of their formation to be assessed over a greater temperature range than was the case for (μ-P)**3**<sub>2</sub>. The three reactions corresponding to eqs 9–11 are very clean (Figures 2, S10, S11) and have a second-order process as the rate-limiting step. Eyring plots are shown in Figure S12, second-order rate constants and activation parameters are summarized in Table 1.

The condensation reaction between molybdaziridine-hydride **1** and corresponding terminal phosphide **2**-P is faster than that between **1** and P<sub>4</sub>, indicating that the formation of μ-phosphide complex (μ-P)**2**<sub>2</sub> is not rate-limiting in the activation of P<sub>4</sub> by **1**. This parallels the reactivity of *tert*-butyl substituted complex **3**, such that in both cases, phosphide bridge formation by condensation of a terminal phosphide entity with an unsaturated metal complex is kinetically plausible to be operative as a post rate-determining step in P<sub>4</sub> activation. Such atom-bridge forming reactions, occurring in concert with inner-sphere electron transfer, have been referred to as “incomplete atom transfer” reactions.<sup>46</sup>

It is instructive to note that the unsymmetrical μ-phosphide complex **3**(μ-P)**2** can be formed cleanly by two different

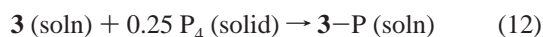
(44) Johnson, A. R.; Cummins, C. C.; Gambarotta, S. *Inorg. Synth.* **1998**, *32*, 123–132.

(45) Iwanura, H.; Mislow, K. *Acc. Chem. Res.* **1988**, *21*, 175–182.

(46) Holm, R. H. *Chem. Rev.* **1987**, *87*, 1401–1449.

condensation reactions (eqs 10 and 11). By far the faster of these two reactions is that between *tert*-butyl-substituted three-coordinate **3** and the *iso*-propyl-substituted terminal phosphide complex **2**-P (eq 10); this reaction is associated with a very small activation enthalpy and a large negative activation entropy ( $\Delta H^\ddagger = 2.7 \pm 0.4 \text{ kcal}\cdot\text{mol}^{-1}$ ,  $\Delta S^\ddagger = -33 \pm 4 \text{ eu}$ ), the latter being quite typical of an associative process. Approaching the same  $3(\mu\text{-P})_2$  product from the other direction, by reaction of molybdaziridine-hydride **1** with terminal phosphide **3**-P, is a process having a considerably higher activation enthalpy ( $\Delta H^\ddagger = 8.7 \pm 0.5 \text{ kcal}\cdot\text{mol}^{-1}$ ,  $\Delta S^\ddagger = -22 \pm 4 \text{ eu}$ ). This sharp contrast can be taken once again to reflect the requirement for substantial reorganization of the molybdaziridine-hydride **1** as it rearranges to its isomer **2** concomitant with substrate binding. The process is analogous to isocyanide binding by **1** and **3**, kinetic studies of which were reported previously.<sup>13</sup> The binding of 1-adamantyl isocyanide (AdNC) by **1** is associated with activation parameters ( $\Delta H^\ddagger = 4.5 \pm 0.5 \text{ kcal}\cdot\text{mol}^{-1}$ ,  $\Delta S^\ddagger = -24 \pm 4 \text{ eu}$ )<sup>13</sup> quite reminiscent of those observed here for its binding of terminal phosphide complexes **2**-P and **3**-P. In line with our mechanistic inferences, the most negative activation entropy is found for formation of the most crowded system,  $(\mu\text{-P})_3$ , and the lowest enthalpy of activation is for attack by the three-coordinate complex **3** on the least hindered terminal phosphide, **2**-P.

**Solution Calorimetry Measurements.** The reaction of three-coordinate **3** with  $\text{P}_4$  giving terminal phosphide **3**-P was measured using an excess of metal complex and solid  $\text{P}_4$ ; the reaction enthalpy for this process is given in eq 12.

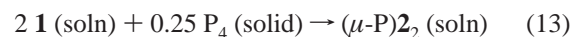


$$\Delta H = -19.5 \pm 0.7 \text{ kcal}\cdot\text{mol}^{-1}$$

Surprisingly, no literature data for the enthalpy of solution of white phosphorus in aromatic solvents could be found. The reported enthalpy of solution of  $\text{P}_4$  in carbon disulfide is 2.0 kcal/mol.<sup>47</sup> Measurement of the enthalpy of solution of  $\text{P}_4$  in toluene yielded a value of  $2.8 \pm 0.1 \text{ kcal}\cdot\text{mol}^{-1}$ . Correction of eq 12 by subtraction of 1/4 the molar enthalpy of solution of  $\text{P}_4$  in toluene yields an enthalpy of reaction 12 with all species in solution of  $-20.2 \text{ kcal}\cdot\text{mol}^{-1}$ . The enthalpy of reaction 4 can be used to generate an estimate for the  $\text{P}=\text{Mo}(\text{N}[\textit{t}\text{-Bu}]\text{Ar})_3$  (**3**-P) bond strength in solution of 92.2 kcal/mol. For these nonpolar reactions it is expected that solvation energies will play only a minor role in the solution thermochemistry and that there is little difference between enthalpies of reaction in toluene solution and in the gas phase. This value is in reasonable agreement with quantum chemical calculations discussed below. The experimental bond enthalpy in solution is considerably lower than that reported earlier<sup>73</sup> for other multiple bonds to Mo in this system, notably  $\text{N}=\text{Mo}(\text{N}[\textit{t}\text{-Bu}]\text{Ar})_3$  (155 kcal·mol<sup>-1</sup>),  $\text{O}=\text{Mo}(\text{N}[\textit{t}\text{-Bu}]\text{Ar})_3$  (156 kcal·mol<sup>-1</sup>), and  $\text{S}=\text{Mo}(\text{N}[\textit{t}\text{-Bu}]\text{Ar})_3$  (104 kcal·mol<sup>-1</sup>). It is interesting that these terminal multiple bond enthalpies diminish in accord with the electronegativity trend for the O, N, S, and P substituent atoms.

For molybdaziridine-hydride complex **1** the reaction with  $\text{P}_4$  is more complex since the  $\mu$ -phosphide complex  $(\mu\text{-P})_2$  or

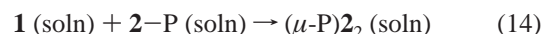
the *cyclo*- $\text{P}_3$  complex **2**- $\text{P}_3$  can be formed depending upon the conditions. The enthalpy of reaction of  $\text{P}_4$  with a large excess of complex **1** could be measured as shown in eq 13.



$$\Delta H = -30.0 \pm 1.2 \text{ kcal}\cdot\text{mol}^{-1}$$

This value is corrected to  $-30.7 \pm 1.2 \text{ kcal}\cdot\text{mol}^{-1}$  with all species in solution by subtraction of 1/4 the enthalpy of solution of  $\text{P}_4$  in toluene. The more exothermic enthalpy of  $\text{P}_4$  addition to **1** as compared with three-coordinate **3** is due to formation of the  $\mu$ -phosphide dinuclear product. In effect, a terminal  $\text{Mo}\equiv\text{P}$  triple bond is not worth as much, energetically, as the sum of two double bonds ( $\text{Mo}=\text{P}=\text{Mo}$ ) found in the dinuclear complex.

A component of the reaction represented by eq 13 could be measured directly:



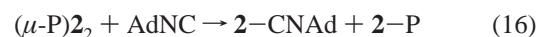
$$\Delta H = -19.4 \pm 1.2 \text{ kcal}\cdot\text{mol}^{-1}$$

The exothermicity of the condensation (eq 14) leading to  $\mu$ -phosphide  $(\mu\text{-P})_2$  could be compared with that obtained previously for the binding of AdNC by **1**:



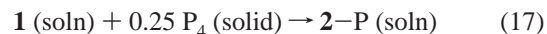
$$\Delta H = -24.6 \pm 0.5 \text{ kcal}\cdot\text{mol}^{-1}$$

This both reveals that AdNC is a better ligand than is terminal phosphide **2**-P for the trisanilide fragment **2**, and suggests that AdNC should be capable of phosphide bridge cleavage as represented by eq 16.



$$\Delta H = -4.1 \pm 0.6 \text{ kcal}\cdot\text{mol}^{-1}$$

Indeed, the phosphide bridge cleavage reaction with adamantyl isocyanide (eq 16) was found to proceed quantitatively and with the measured reaction enthalpy as shown. Subtraction of eq 16 from eq 15 yields an independent value of  $-20.5 \pm 1.1 \text{ kcal}\cdot\text{mol}^{-1}$  for the enthalpy of formation of  $\mu$ -phosphide complex  $(\mu\text{-P})_2$  as shown in eq 14. The average value of  $-20 \pm 1.5 \text{ kcal/mol}$  is accepted for the enthalpy of formation of dinuclear complex  $(\mu\text{-P})_2$  by the condensation reaction shown in eq 14. Note that it is important whenever possible to check independently data on enthalpies of reaction of such air-sensitive complexes.



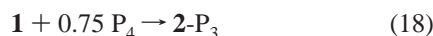
$$\Delta H = -10.7 \pm 2.7 \text{ kcal}\cdot\text{mol}^{-1}$$

Now, subtracting the reaction enthalpy value obtained for eq 14 (phosphide-bridge formation) from that obtained for 13 ( $\text{P}_4$  activation by **1** giving phosphide bridge) gives a value, shown in eq 17, for cleavage of  $\text{P}_4$  by **1** yielding *terminal* phosphide **2**-P. This enthalpy of reaction is found to be  $9.5 \pm 3.4 \text{ kcal}\cdot\text{mol}^{-1}$  less exothermic than that for terminal phosphide formation from reaction of  $\text{P}_4$  with *tert*-butyl substituted three-coordinate **3** (equation 12). This implies that in the formal definition of bond strength the value for **2**-P (82.7 kcal·mol<sup>-1</sup>)

(47) Wagman, D. D.; United States National Bureau of Standards; American Chemical Society; American Institute of Physics. *The NBS tables of chemical thermodynamic properties: selected values for inorganic and C1 and C2 organic substances in SI units*; American Chemical Society and the American Institute of Physics for the National Bureau of Standards: New York; Washington, DC, 1982.

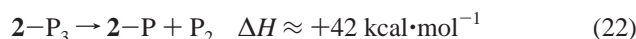
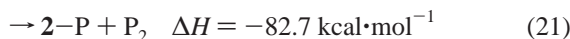
is weaker than that for **3**-P (92.2 kcal·mol<sup>-1</sup>). It should be noted that the enthalpy of binding of AdNC to **1** was similarly found to be less exothermic than binding to **3**.<sup>13</sup> That observation was ascribed to the energetics of molybdaziridine-hydride **1** isomerization to trisanilide **2**, for which  $\Delta H_{\text{isom}} \cong +5 \pm 2$  kcal·mol<sup>-1</sup>. The current estimate of  $\Delta H_{\text{isom}}$  (**1**→**2**) based on P<sub>4</sub> reaction enthalpies is somewhat higher, but not outside the overlap of experimental error. It must also be considered as possible that due to the steric and electronic differences between binding of AdNC compared to P this difference is not simply due to experimental errors but instead reflective of a real, albeit small, difference in binding energies to **2** as compared with **3**, for AdNC versus P.

Also studied by solution calorimetry was the clean and quantitative reaction described by eq 7 above, namely the consumption of **2**-P<sub>3</sub> by 5 equiv of **1**, providing 3 equiv of ( $\mu$ -P)<sub>2</sub>. With all species in solution  $\Delta H$  for this reaction was found to be  $-67.2 \pm 1.3$  kcal·mol<sup>-1</sup>. Interestingly, subtraction of eq 7 from three times eq 13 yields directly eq 18:



$$\Delta H = -24.9 \pm 4.9 \text{ kcal}\cdot\text{mol}^{-1}$$

Using enthalpy of formation data mentioned earlier, the enthalpy of  $3/4 \text{P}_4 \rightarrow \text{P}_3$  is calculated to be  $+48.8$  kcal·mol<sup>-1</sup>, yielding an estimated  $\eta^3\text{-P}_3\text{-Mo}$  bond enthalpy of  $74$  kcal·mol<sup>-1</sup>. The fact that this bond strength estimate is actually weaker than the P≡Mo bond strength estimate in **2**-P of  $82.7$  kcal·mol<sup>-1</sup> does not, however, imply that extrusion of P<sub>2</sub> or even  $1/2 \text{P}_4$  from the  $\eta^3\text{-P}_3$  complex would be spontaneous. For example, the sequence represented in eqs 19–22 shows that P<sub>2</sub> extrusion from the  $\eta^3\text{-P}_3$  complex **2**-P<sub>3</sub> is endothermic by ca.  $42$  kcal·mol<sup>-1</sup>.

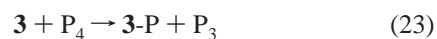


A similar sequence one might envision for **2**-P<sub>3</sub> is extrusion of  $1/2 \text{P}_4$  with formation of **2**-P. This would be less endothermic by  $27.4$  kcal/mol (half the enthalpy of reaction 1) and hence endothermic by only  $\approx 15$  kcal/mol. Considering that extrusion of  $1/2 \text{P}_4$  should be entropically favored, the  $\eta^3\text{-P}_3$  complex **2**-P<sub>3</sub> is estimated to be of marginal thermodynamic stability with respect to formation of **2**-P and  $1/2 \text{P}_4$ . It is therefore not surprising that the corresponding  $\eta^3\text{-P}_3$  complex of the *tert*-butyl-substituted system **3**, where less room is available in the ligand-binding pocket, has not been detected. It should be emphasized that this analysis includes errors on the order of  $\approx 5$  kcal·mol<sup>-1</sup> based on both the experimental data reported here, but also in the enthalpy of formation of P<sub>3</sub>(g) itself.

**Initial Mechanistic Conclusions.** The investigation reported herein has as its main point elucidation of the mechanism of P<sub>4</sub> activation and cleavage by three-coordinate **3** and by molybdaziridine-hydride **1**. Unfortunately, while we now know that in both cases the reaction is first-order both in metal complex and in P<sub>4</sub>, the multiple steps that must transpire after initial P<sub>4</sub>

binding and en route to  $\mu$ -phosphide, terminal phosphide, or *cyclo*-P<sub>3</sub> product formation are post rate-determining. Intermediate complexes are not observed. We also know that the *cyclo*-P<sub>3</sub> complex seen exclusively for the less-hindered *iso*-propyl-substituted system, is not an intermediate in the formation of terminal or bridged phosphide systems. Finally, our studies establish that formation of  $\mu$ -phosphide products by condensation of 1 equiv of a terminal phosphide with 1 equiv of **1** or **3** is sufficiently fast to constitute the terminal post rate-determining step of P<sub>4</sub> activation.

While the kinetic studies establish binding of P<sub>4</sub> at a single Mo center as the rate-determining step in the activation process, a central issue is whether subsequent steps require intervention of a second equivalent of metal complex per P<sub>4</sub> molecule (bimetallic activation) or whether a single metal site is sufficient for P<sub>4</sub> breakdown to the observed phosphide products.



$$\Delta H = +29 \text{ kcal}\cdot\text{mol}^{-1}$$

Using the value determined above of  $\approx 92$  kcal·mol<sup>-1</sup> for the Mo≡P triple bond energy in **3**-P together with the enthalpy of eq 2, we see that P-atom abstraction from P<sub>4</sub> by **3** as in eq 23 is endothermic by ca.  $29$  kcal·mol<sup>-1</sup>. While differing in terms of magnitude, computational studies presented below will affirm the conclusion that single-metal P-atom abstraction from P<sub>4</sub> is ruled out on the basis of thermochemistry, in view of the low activation energy (Table 1) for the reaction of P<sub>4</sub> with either **1** or **3**.

**Computational Studies.** All calculations were carried out using the Amsterdam Density Functional (ADF) program package,<sup>48,49</sup> version 2004.01.<sup>50</sup> The local exchange-correlation potential of Vosko et al.<sup>51</sup> (VWN) was augmented self-consistently with gradient-corrected functionals for electron exchange according to Becke,<sup>52</sup> and electron correlation according to Perdew.<sup>53,54</sup> This nonlocal density functional is termed BP86 in the literature and has been shown to give excellent results both for the geometries and for the energetics of transition metal systems.<sup>55</sup> Relativistic effects were included using the zero-order regular approximation (ZORA).<sup>56,57</sup> The basis set used was the ADF ZORA/TZ2P (triple- $\zeta$  with two polarization functions) basis.

(48) te Velde, G.; Bickelhaupt, F. M.; Baerends, E. J.; Fonseca Guerra, C.; van Gisbergen, S. J. A.; Snijders, J. G.; Ziegler, T. *J. Comput. Chem.* **2001**, *22*, 931–967.

(49) Fonseca Guerra, C.; Snijders, J. G.; te Velde, G.; Baerends, E. J. *Theor. Chem. Acc.* **1998**, *99*, 391–403.

(50) Baerends, E. J.; Autschbach, J.; Bérces, A.; Bo, C.; Boerrigter, P. M.; Cavallo, L.; Chong, D. P.; Deng, L.; Dickson, R. M.; Ellis, D. E.; Fan, L.; Fischer, T. H.; Fonseca Guerra, C.; van Gisbergen, S. J. A.; Groeneveld, J. A.; Gritsenko, O. V.; Grüning, M.; Harris, F. E.; van den Hoek, P.; Jacobsen, H.; van Kessel, G.; Kootstra, F.; van Lenthe, E.; McCormack, D. A.; Osinga, V. P.; Patchkovskii, S.; Philipsen, P. H. T.; Post, D.; Pye, C. C.; Ravenek, W.; Ros, P.; Schipper, P. R. T.; Schreckenbach, G.; Snijders, J. G.; Sola, M.; Swart, M.; Swerhone, D.; te Velde, G.; Vermooijs, P.; Versluis, L.; Visser, O.; van Wezenbeek, E.; Wiesenekker, G.; Wolff, S. K.; Woo, T. K.; Ziegler, T. ADF2004.01 ed.; Theoretical Chemistry, Vrije Universiteit, Amsterdam, The Netherlands, <http://www.scm.com>, 2004.

(51) Vosko, S. H.; Wilk, L.; Nusair, M. *Can. J. Phys.* **1980**, *58*, 1200–1211.

(52) Becke, A. D. *Phys. Rev. A* **1988**, *38*, 3098–3100.

(53) Perdew, J. P. *Phys. Rev. B* **1986**, *33*, 8822–8824.

(54) Perdew, J. P. *Phys. Rev. B* **1986**, *34*, 7406–7406.

(55) Deng, L. Q.; Schmid, R.; Ziegler, T. *Organometallics* **2000**, *19*, 3069–3076.

(56) van Lenthe, E.; Baerends, E. J.; Snijders, J. G. *J. Chem. Phys.* **1993**, *99*, 4597–4610.

(57) van Lenthe, E.; Snijders, J. G.; Baerends, E. J. *J. Chem. Phys.* **1996**, *105*, 6505–6516.

Shown in Figure 3 are 16 molecular structures optimized in the course of potential energy surface exploration for P<sub>4</sub> activation by model molybdenum complex Mo(NH<sub>2</sub>)<sub>3</sub>. All depicted structures were found to have zero negative vibrational frequencies, revealing them to be minima on the potential energy surface. The discussion of energetics in this section includes zero-point energy corrections. While the structures in Figure 3 do not take into account the substantial steric influences of the N(*i*-Pr)Ar or N(*t*-Bu)Ar ligands in the experimentally studied systems, the model system provides a stepping-off point for discussion of microscopic steps that make up the P<sub>4</sub>-activation mechanism.

The initial binding event, which also is the RDS for P<sub>4</sub>-activation, is likely to be coordination of P<sub>4</sub> in an η<sup>1</sup> fashion. In Figure 3 this is the reaction **Mo** + P<sub>4</sub> → **MoP<sub>4</sub>-a**, the calculated exothermicity of which is 8 kcal·mol<sup>-1</sup>. Note that trigonal-planar **Mo** was optimized in its quartet ground state using the spin-unrestricted formalism employed for all open-shell systems in this study. No symmetry restrictions were imposed, and this is an important point because in many cases the orientation of the NH<sub>2</sub> hydrogens is seen to correlate with the spin state. The **MoP<sub>4</sub>-a** structure was optimized in its doublet ground state. In **MoP<sub>4</sub>-a**, one NH<sub>2</sub> ligand (that on the right in Figure 3) is rotated such that its N p-orbital based lone pair is coplanar with the Mo–P vector, producing a pseudo-C<sub>s</sub> as opposed to a pseudo-C<sub>3</sub> molecular structure. The Mo–P bond length is 2.322 Å, while the P–P distances fall in the range 2.21–2.26 Å. By way of comparison, the P–P bond length in P<sub>4</sub> is calculated at 2.222 Å.

While the intact tetrahedral P<sub>4</sub> molecule has been seen to behave as a simple η<sup>1</sup> ligand in nickel(0),<sup>58</sup> tungsten(0),<sup>59</sup> and iron(II) systems,<sup>60</sup> it is also known to bind to rhodium(I)<sup>61,62</sup> and monovalent group 11 ions<sup>63,64</sup> as an η<sup>2</sup> ligand. For this reason, optimization was also carried out for an η<sup>2</sup> adduct between P<sub>4</sub> and **Mo**. This converged to a structure **MoP<sub>4</sub>-c** in which the Mo center has clearly inserted into one edge of the P<sub>4</sub> tetrahedron. This structure lies 13 kcal·mol<sup>-1</sup> below that of the η<sup>1</sup> adduct **MoP<sub>4</sub>-a**. In the experimental system an intermediate corresponding to **MoP<sub>4</sub>-c** cannot be ruled out, but likely is disfavored by steric influences not accounted for in the computational model. Systems in which a metal complex has inserted into a single edge of the P<sub>4</sub> tetrahedron have been described in the literature.<sup>65,66</sup>

One reaction mode of interest has to do with the issue of the capability of an MoL<sub>3</sub> complex to abstract a single phosphorus atom from P<sub>4</sub>, generating the P<sub>3</sub> doublet radical in the process. This was explored computationally via **MoP<sub>4</sub>-b**, a P<sub>3</sub>-substituted doublet phosphinidene structure that lies only 4 kcal·mol<sup>-1</sup> in energy higher than η<sup>1</sup> adduct **MoP<sub>4</sub>-a**. The Mo–P multiple bond in intermediate **MoP<sub>4</sub>-b** is associated with an Mo–P interatomic

distance of 2.234 Å, and the P–P double bond in the P<sub>3</sub> substituent with a distance of 2.038 Å. Fragmentation of **MoP<sub>4</sub>-b** into singlet terminal phosphide **MoP** and <sup>2</sup>[P<sub>3</sub>], **P<sub>3</sub>**, is calculated to be uphill by 14 kcal·mol<sup>-1</sup>. Overall, the abstraction reaction **Mo** + P<sub>4</sub> → **MoP** + **P<sub>3</sub>** is uphill by ca. 9 kcal·mol<sup>-1</sup>. We can compare this number to that obtained as described above through thermochemical measurements. The difference between the measured Mo–P triple bond enthalpy for **3**–P of 92.2 kcal·mol<sup>-1</sup> and the P<sub>4</sub> → P + P<sub>3</sub> fragmentation enthalpy (eq 2) of 120.9 kcal·mol<sup>-1</sup> gives a P-atom abstraction enthalpy of +27.8 kcal·mol<sup>-1</sup>. This value is greater, by 18.8 kcal·mol<sup>-1</sup>, than that emerging from the computational study. More than half of this discrepancy can be traced to the Mo–P triple bond enthalpy, the calculated value for which is 102 kcal·mol<sup>-1</sup>. If the thermochemical data for P<sub>4</sub> → P + P<sub>3</sub> (eq 2) from the literature are substantially in error, this might be another factor contributing to the discrepancy. Our calculated value for this reaction is +111 kcal·mol<sup>-1</sup>, accounting for the remainder of the disconnect in the experimental versus computational estimates of the capability of MoL<sub>3</sub> to abstract P-atom from P<sub>4</sub>. In all cases the P<sub>4</sub>, P-atom, and cyclo-P<sub>3</sub> fragments are calculated in their ground singlet, quartet, and doublet states, respectively.

As a matter of note, the correct ground-state structure of the P<sub>3</sub> radical needs to be utilized in the computations in order for the foregoing conclusions to have merit. While at least one recent publication takes the P<sub>3</sub> radical to have a linear, *D*<sub>∞h</sub>, geometry,<sup>67</sup> the accepted ground state for P<sub>3</sub> is a triangle of *C*<sub>2v</sub> symmetry.<sup>68</sup> Our own calculations show the *C*<sub>2v</sub> structure to lie lower in energy than the *D*<sub>∞h</sub> geometry, by some 28 kcal·mol<sup>-1</sup>. As a check on the quality of our calculations, note that our calculated value for eq 1 (P<sub>4</sub> → 2 P<sub>2</sub>) is 54.4 kcal·mol<sup>-1</sup>, essentially perfect agreement with the experimental number. Other computational studies of P<sub>n</sub> clusters have similarly used the P<sub>4</sub> → 2 P<sub>2</sub> reaction as a benchmark.<sup>69</sup>

The capture of <sup>2</sup>[P<sub>3</sub>] by an MoL<sub>3</sub> complex to form (η<sup>3</sup>-P<sub>3</sub>)-MoL<sub>3</sub> is modeled by the reaction **Mo** + P<sub>3</sub> → **MoP<sub>3</sub>-b**, calculated to be downhill by 80 kcal·mol<sup>-1</sup>. This number compares well with that determined above for the Mo–P<sub>3</sub> bond enthalpy in **2**–P<sub>3</sub> of 74 kcal·mol<sup>-1</sup>. But since the molybdenum complexes are not thermochemically competent to effect P-atom abstraction from P<sub>4</sub>, complexes of the type **MoP<sub>3</sub>-b** are not likely to be formed from simple P<sub>3</sub> capture.

Since **MoP<sub>4</sub>-b** is only slightly more energetic than the η<sup>1</sup>-P<sub>4</sub> complex **MoP<sub>4</sub>-a**, its reaction with **Mo** to produce **MoP** and **MoP<sub>3</sub>-b** provides a good explanation for cyclo-P<sub>3</sub> complex formation. This bimetallic reaction channel is downhill by 67 kcal·mol<sup>-1</sup>.

Double radical addition to P<sub>4</sub> to produce closed-shell tetraphosphabicyclobutane<sup>70</sup>-type products structurally analogous to **Mo<sub>2</sub>P<sub>4</sub>-a** are well-documented in the literature.<sup>71</sup> This is so also for substituents including N(SiMe<sub>3</sub>)<sub>2</sub><sup>70</sup> and 2,4,6-*t*-Bu<sub>3</sub>C<sub>6</sub>H<sub>2</sub>.<sup>72</sup> The structure represented by **Mo<sub>2</sub>P<sub>4</sub>-a** is the lowest-lying

(58) Dapporto, P.; Midollini, S.; Sacconi, L. *Angew. Chem., Int. Ed. Engl.* **1979**, *18*, 469–469.

(59) Groer, T.; Baum, G.; Scheer, M. *Organometallics* **1998**, *17*, 5916–5919.

(60) de los Rios, I.; Hamon, J. R.; Hamon, P.; Lapinte, C.; Toupet, L.; Romerosa, A.; Peruzzini, M. *Angew. Chem., Int. Ed.* **2001**, *40*, 3910.

(61) Lindsell, W. E.; McCullough, K. J.; Welch, A. J. *J. Am. Chem. Soc.* **1983**, *105*, 4487–4489.

(62) Lindsell, W. E. *Chem. Commun.* **1982**, 1422–1424.

(63) Tai, H. C.; Krossing, I.; Seth, M.; Deubel, D. V. *Organometallics* **2004**, *23*, 2343–2349.

(64) Krossing, I.; van Wullen, L. *Chem. Eur. J.* **2002**, *8*, 700–711.

(65) Scherer, O. J.; Swarowsky, M.; Swarowsky, H.; Wolmershauser, G. *Angew. Chem., Int. Ed. Engl.* **1988**, *27*, 694–695.

(66) Scherer, O. J.; Swarowsky, M.; Wolmershauser, G. *Organometallics* **1989**, *8*, 841–842.

(67) Guo, L.; Wu, H. C.; Jin, Z. H. *J. Mol. Struct. (THEOCHEM)* **2004**, *677*, 59–66.

(68) Balasubramanian, K.; Sumathi, K.; Dai, D. G. *J. Chem. Phys.* **1991**, *95*, 3494–3505.

(69) Haser, M.; Treutler, O. *J. Chem. Phys.* **1995**, *102*, 3703–3711.

(70) Niecke, E.; Ruger, R.; Krebs, B. *Angew. Chem., Int. Ed. Engl.* **1982**, *21*, 544–545.

(71) Bezombes, J. P.; Hitchcock, P. B.; Lappert, M. F.; Nycz, J. E. *Dalton Trans.* **2004**, 499–501.

(72) Riedel, R.; Hausen, H. D.; Fluck, E. *Angew. Chem., Int. Ed. Engl.* **1985**, *24*, 1056–1057.



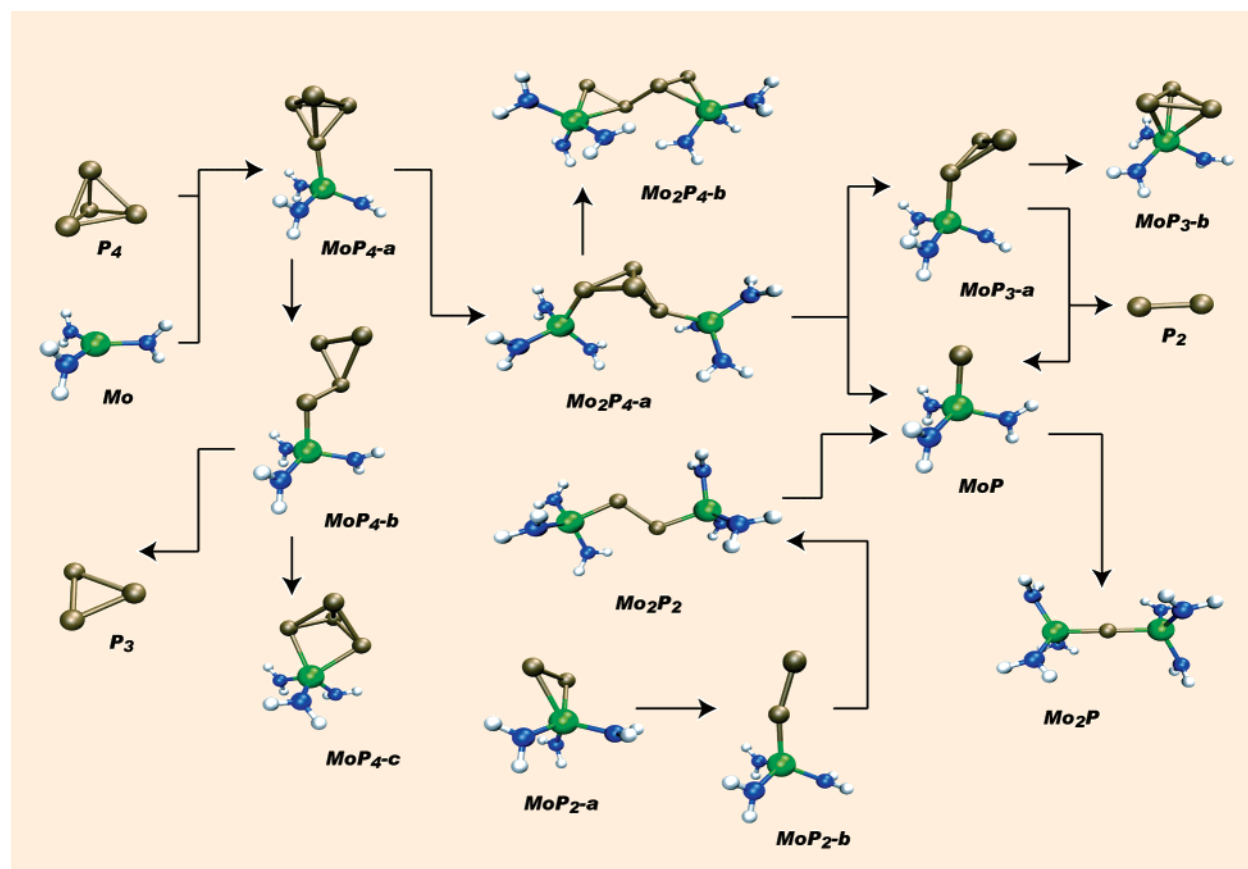
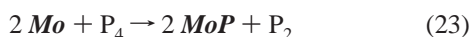


**Figure 3.** Structures optimized computationally in considering the P<sub>4</sub> activation mechanism and corresponding thermochemistry. Arrows drawn in the figure are merely suggestive of possible reaction pathways. All depicted structures were shown to be potential energy minima. See text for details.

minimum we were able to locate for the 2 Mo + P<sub>4</sub> system, lying 16 kcal·mol<sup>-1</sup> below an alternative structure *Mo<sub>2</sub>P<sub>4</sub>-b* in which the P<sub>4</sub> molecule has opened into a *trans*-butadiene-like bridging ligand. Addition of 2 Mo to P<sub>4</sub> producing singlet *Mo<sub>2</sub>P<sub>4</sub>-a* is downhill by 43 kcal·mol<sup>-1</sup>.

From *Mo<sub>2</sub>P<sub>4</sub>-a*, fragmentation to 2 *MoP* + P<sub>2</sub> is an attractive, productive reaction channel that is only uphill by ca. 10 kcal·mol<sup>-1</sup>. Such a fragmentation may be entropically driven, given the conversion of one molecule into three. Related to this is an alternative conceivable fragmentation of *Mo<sub>2</sub>P<sub>4</sub>-a*, to *MoP* together with singlet *MoP<sub>3</sub>-a*, a reaction channel uphill by only 12 kcal·mol<sup>-1</sup>. This suggests the overall sequence given in eq 23 and which may proceed via intermediates *Mo<sub>2</sub>P<sub>4</sub>-a* and *MoP<sub>3</sub>-a*. Also, if *MoP<sub>3</sub>-a* is formed and does not fragment it may close to singlet *MoP<sub>3</sub>-b*, a process favorable by 41 kcal·mol<sup>-1</sup>.



$$\Delta H = -32.5 \text{ kcal}\cdot\text{mol}^{-1}$$

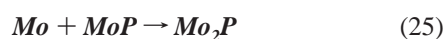
With molecular P<sub>2</sub> as a possible intermediate as suggested in eq 23, one may propose rapid capture of P<sub>2</sub> to form 1:1 and 1:2 complexes with molybdenum. The binding of P<sub>2</sub> by Mo to form the 1:1  $\eta^2$  doublet adduct *MoP<sub>2</sub>-a* is downhill by 43 kcal·mol<sup>-1</sup> and more favorable by 13 kcal·mol<sup>-1</sup> than is binding in an  $\eta^1$  fashion (doublet *MoP<sub>2</sub>-b*). Both experimental fragments 2 and 3 are known in certain cases to be able to bind alkynes<sup>20</sup> and nitriles,<sup>21</sup> respectively, in an  $\eta^2$  fashion, so  $\eta^2$ -binding of P<sub>2</sub> should not be sterically out of the question in the experimental systems.

Binding of P<sub>2</sub> by 2 equiv of Mo is also energetically favorable. Since the  $\mu$ -dinitrogen complex ( $\mu$ : $\eta^1, \eta^1$ -N<sub>2</sub>)**3**, an intermediate in N<sub>2</sub> splitting by complex **3**,<sup>23</sup> has a linear bridging mode for the  $\mu$ -dinitrogen ligand and a triplet ground state, a similar structure and a triplet electronic state was employed in the optimization of *Mo<sub>2</sub>P<sub>2</sub>*. As shown in Figure 3, the structure of *Mo<sub>2</sub>P<sub>2</sub>* converged to a zigzag shape with bond angles at phosphorus of 113° and 115°, a P–P bond length of 2.16 Å suggestive of an approximate 1.5 bond order, and P–Mo distances of ca. 2.25 Å consistent with multiple bond character. Interestingly, the two Mo centers in the calculated structure of *Mo<sub>2</sub>P<sub>2</sub>* are not equivalent, one having its two d-electrons paired, the other responsible for the molecular triplet state; +4 is the best oxidation state assignment for both Mo centers in *Mo<sub>2</sub>P<sub>2</sub>*. The exothermicity of *Mo<sub>2</sub>P<sub>2</sub>* formation is 74.5 kcal·mol<sup>-1</sup>, this large downhill value being reflective of the intrinsic high energy of the quartet Mo complex and also the P<sub>2</sub> molecule. Further cleavage of *Mo<sub>2</sub>P<sub>2</sub>* to two equiv of *MoP* is downhill by another 12.5 kcal·mol<sup>-1</sup>. As presented in eq 24, the overall consumption of P<sub>2</sub> by molybdenum, and conversion into 2 equiv of terminal phosphide is energetically quite favorable. The analogous process in the case of N<sub>2</sub> is also downhill, and interestingly, by a very similar amount. Using the experimental MoN triple bond energy for **3**-N<sup>73</sup> and 226 kcal·mol<sup>-1</sup> for the N<sub>2</sub> BDE, the splitting of N<sub>2</sub> by 2 equiv of **3** giving 2 equiv of **3**-N is downhill by 84.6 kcal·mol<sup>-1</sup>.



$$\Delta H = -87.0 \text{ kcal}\cdot\text{mol}^{-1}$$

As reported above in the sections devoted to kinetic and thermochemical measurements, it is favorable to form  $\mu$ -phosphide bridged complexes by combination of **1** or **3** with terminal phosphide complexes **2**-P or **3**-P. This is modeled computationally by eq 25. Note that the structure of  $\text{Mo}_2\text{P}$  was computed in a doublet electronic state and with imposition of  $C_i$  symmetry, as observed experimentally for such phosphide-bridged dinuclear systems.<sup>26,43</sup> The Mo-P bond distance in  $\text{Mo}_2\text{P}$  is 2.213 Å, while the corresponding distance for the experimental analogue  $(\mu\text{-P})[\text{Mo}(\text{N}[\textit{t}\text{-Bu}]\text{Ph})_3]_2$  characterized structurally by X-ray diffraction was 2.2430(6) Å.<sup>43</sup> The *iso*-propyl substituted complex **2**- $\mu$ -P was also crystallographically characterized and found to have a center of symmetry at the bridging phosphorus atom; in this case the Mo-P distance was 2.2164(4) Å.<sup>26</sup> Other structurally characterized neutral complexes in which a single phosphorus atom bridges two identical metal complexes are known for tungsten<sup>74</sup> and for zirconium.<sup>75,76</sup>



$$\Delta H = -28.1 \text{ kcal}\cdot\text{mol}^{-1}$$

Because of the extreme steric repulsions present in the equatorial belt of the single atom-bridged systems  $(\mu\text{-P})_2$  or  $(\mu\text{-P})_3$ , these would be expected to form with less exothermicity than the  $-28.1 \text{ kcal}\cdot\text{mol}^{-1}$  calculated for the model system in eq 25. Experimental data shown in eq 14 bear this out, as the enthalpy of formation of  $(\mu\text{-P})_2$  in solution ( $-19.4 \text{ kcal/mol}$ ) is in fact less exothermic than the calculated value. The more sterically demanding *tert*-butyl ligand system in  $(\mu\text{-P})_3$  forms only at low temperature, but its enthalpy of formation as extracted from VT-NMR measurements (see above) is essentially identical to that determined by solution calorimetry for  $(\mu\text{-P})_2$ . The diminished tendency for  $\mu$ -phosphide bridge formation in the case of more hindered **3** can thus be ascribed exclusively to entropy considerations. The value of  $-28.1 \text{ kcal}\cdot\text{mol}^{-1}$  may represent a maximum upper bound on  $\Delta H$  for forming such P-atom bridged complexes. Entropic terms disfavor formation of phosphide-bridged complexes in which

the ancillary ligands are locked into a restricted conformational arrangement.

### Concluding Remarks

Molecular phosphorus ( $\text{P}_4$ ) activation is an important prerequisite to the synthesis of organic  $\text{P}_1$  derivatives. Recent work has shown that  $\text{P}_1$  organic compounds, in particular phosphalkynes ( $\text{R}-\text{C}\equiv\text{P}$ ),<sup>77-81</sup> can be obtained through the emerging chemistry of terminal phosphide ( $\text{L}_n\text{M}\equiv\text{P}$ ) complexes.<sup>82</sup> The present work has focused on mechanistic issues associated with the production of terminal phosphide complexes of molybdenum by reaction of  $\text{P}_4$  with reactive trivalent molybdenum trisamides. While all steps (other than the initial  $\text{P}_4$  binding event) in what must be a complex multistep mechanism are post rate-determining, it was possible to rule out the straightforward abstraction of a phosphorus atom from  $\text{P}_4$ , since this reaction is shown thermochemically and computationally to be associated with a barrier so high as to be inconsistent with the low observed  $\text{P}_4$  activation energy. On the basis of computational results, it is suggested that two routes to the terminal phosphide functional group may be operative in parallel. The first of these is bimetallic splitting of  $\text{P}_4$  in a manner that generates 2 equiv of terminal phosphide along with  $\text{P}_2$ . The second is the bimetallic binding and splitting of the  $\text{P}_2$  so generated to produce another 2 equiv of terminal phosphide, a process quite analogous to the known splitting of  $\text{N}_2$  by complexes **1**<sup>12,25</sup> and **3**.<sup>22-25</sup>

**Acknowledgment.** The authors thank the United States National Science Foundation for funding via Grant CRC-0209977, and C.C.C. is thankful also for funding via CHE-0316823. The authors also thank Dr. George Fisher of Barry University for a gift of  $\text{P}_4$ .

**Supporting Information Available:** Figures S1 through S12; kinetic traces and Eyring plots stemming from stopped-flow kinetic studies; crystallographic data in CIF format for the structure of  $(\eta^3\text{-P}_3)\text{Mo}(\text{OCy})_3(\text{HN}[\textit{i}\text{-Pr}]\text{Ar})$ ; Cartesian coordinates, relative energies, and zero-point energies for all calculated structures. This material is available free of charge via the Internet at <http://pubs.acs.org>.

JA054253+

- (73) Cherry, J. P. F.; Johnson, A. R.; Baraldo, L. M.; Tsai, Y. C.; Cummins, C. C.; Kryatov, S. V.; Rybak-Akimova, E. V.; Capps, K. B.; Hoff, C. D.; Haar, C. M.; Nolan, S. P. *J. Am. Chem. Soc.* **2001**, *123*, 7271-7286.  
 (74) Scheer, M.; Müller, J.; Schiffer, M.; Baum, G.; Winter, R. *Chem. Eur. J.* **2000**, *6*, 1252-1257.  
 (75) Fermin, M. C.; Ho, J. W.; Stephan, D. W. *J. Am. Chem. Soc.* **1994**, *116*, 6033-6034.  
 (76) Fermin, M. C.; Ho, J. W.; Stephan, D. W. *Organometallics* **1995**, *14*, 4247-4256.

- (77) Nixon, J. F. *Chem. Ind.* **1993**, 404-407.  
 (78) Nixon, J. F. *Chem. Rev.* **1988**, *88*, 1327-1362.  
 (79) Dillon, K. B.; Mathey, F.; Nixon, J. F. *Phosphorus: The Carbon Copy*; Wiley: Chichester, 1998.  
 (80) Regitz, M.; Scherer, O. J., Eds. *Multiple Bonds and Low Coordination in Phosphorus Chemistry*; Thieme: Stuttgart, 1990.  
 (81) Nixon, J. F. *Coord. Chem. Rev.* **1995**, *145*, 201-258.  
 (82) Figueroa, J. S.; Cummins, C. C. *J. Am. Chem. Soc.* **2004**, *126*, 13916-13917.